ELSEVIER

Spectrochimica Acta Part B 62 (2007) 1582–1589

SPECTROCHIMICA ACTA PART B

www.elsevier.com/locate/sab

Towards quantitative laser-induced breakdown spectroscopy analysis of soil samples ☆

B. Bousquet *, J.-B. Sirven [1], L. Canioni

Centre de Physique Moléculaire Optique et Hertzienne, Université Bordeaux 1, 351 cours de la Libération, 33405 Talence Cedex, France

Received 27 November 2006; accepted 11 October 2007
Available online 18 October 2007

Abstract

A quantitative analysis of chromium in soil samples is presented. Different emission lines related to chromium are studied in order to select the best one for quantitative features. Important matrix effects are demonstrated from one soil to the other, preventing any prediction of concentration in different soils on the basis of a univariate calibration curve. Finally, a classification of the LIBS data based on a series of Principal Component Analyses (PCA) is applied to a reduced dataset of selected spectral lines related to the major chemical elements in the soils. LIBS data of heterogeneous soils appear to be widely dispersed, which leads to a reconsideration of the sampling step in the analysis process.

Keywords: LIBS; Analysis; Sorting; Classification; Principal Component Analysis; Matrix effects; Sampling

1. Introduction

Laser-induced breakdown spectroscopy (LIBS) enables one to obtain the atomic emission spectrum of a sample (solid, liquid or gas) [1], from which qualitative and quantitative information on the sample can be derived through an adapted spectra processing. A very common application of LIBS consists in measuring the concentration of a species — the analyte-in a sample from its calibration curve [2], i.e. from the intensity of a related spectral line. For quantitative analysis, other supervised methods have been used to deal with LIBS spectra such as Partial Least-Squares (PLS) regression [3–5] and Artificial Neural Networks (ANN) [6,7]. Both allow taking into account many spectral lines in the processing and ANN is efficient to deal with the nonlinearity of the LIBS signal as a function of the concentration, due to the self-absorption process in dense plasma. In addition, it will be demonstrated below in this paper that all these methods (univariate calibration curve, PLS and ANN), when applied to soils samples, are sensitive to matrix effects, originating from physical and chemical properties changes on the laser-matter interaction from a sample matrix to another one. As a consequence of matrix effects, the final relationship between the LIBS signal and the analyte concentration depends on the matrix of the soil sample. Matrix effects then appear to be a real problem for quantitative LIBS and a way to deal with this problem is to classify the data set in a preliminary step of the analysis. Indeed, matrix effects in soils are mainly due to the physical properties related to the concentration of major elements which constitute the soils, i.e. mainly aluminum, silicon or calcium. Clay presents a high concentration in aluminum and has often the appearance of a very thin powder. Sand, highly concentrated in silicon demonstrates larger size grains. To simplify, it is expected that a series of soils samples containing about the same quantity of aluminum should constitute a first class while those containing about the same quantity of silicon should constitute a second class and so on. But instead of using only the concentrations in aluminum and silicon, the classification proposed here is based

☆ This paper was presented at the 4th International Conference on Laser Induced Plasma Spectroscopy and Applications (LIBS 2006) held in Montreal, Canada, 5–8 September 2006, and is published in the Special Issue of Spectrochimica Acta Part B, dedicated to that conference.

* Corresponding author. Tel.: +33 540002870; fax: +33 540006970.
E-mail addresses: bruno.bousquet@u-bordeaux1.fr (B. Bousquet), jean-baptiste.sirven@cea.fr (J.-B. Sirven).
[1] Present address: CEA Saclay, Département de Physico-Chimie, Service de Chimie Physique, Laboratoire de Réactivité des Surfaces et des Interfaces, Bât. 467-Point Courrier 56, 91191 Gif sur Yvette Cedex, France.

0584-8547/$ - see front matter © 2007 Published by Elsevier B.V.
doi:10.1016/j.sab.2007.10.018

on a multivariate analysis called Principal Component Analysis (PCA). Once this classification proceeded, it is expected that a first quantitative model could be applied for the samples included into the first class, then that a second quantitative model could be applied to the second class and so on. Conversely, if a sample does not belong to any class, it appears to be very difficult to predict the analyte concentration, whatever the supervised method used for quantitative analysis.

Classification of LIBS data can be performed in different ways. The simplest case is binary identification, which can be achieved from a particular spectral line showing a clear intensity enhancement in one case [8]. But if the number of classes increases, more advanced spectra treatments have to be used to discriminate them, such as the measurement of intensity ratios between well-chosen lines [9–12], the comparison to a spectra database, or by using chemometrics techniques such as Artificial Neural Networks [7,13] or Principal Components Analysis (PCA) [14]. PCA has been used for LIBS spectra processing for several years and was shown to achieve good classification ability, particularly in complex cases. Fink et al. [15] applied it to the identification of polymers, Goode et al. [16] performed an efficient sorting of metal alloys, Samek et al. [17] succeeded in the recognition of carious teeth. In the framework of security, Samuels et al. [18] used PCA to separate bacteria from pollens and mushrooms, Munson et al. [19] optimized the PCA by a selection of spectra in order to identify biological aerosols and chemical compounds, and Hybl et al. [20] suggested the potentiality of PCA to distinguish bioaerosols from interferants coming from ambient environment. The same technique was used by Martin et al. [3] to identify treated wood samples.

In this paper, we present quantitative LIBS applied to soil samples, specifically pointing out the matrix effects. Then we propose a method for classifying soils by applying PCA to LIBS data. A selection of relevant spectral lines related to major elements is applied in order to reduce the dimensionality of the dataset. Then a sequential methodology is proposed to separate the whole dataset into different classes. The large variance of data due to heterogeneity of soil samples is finally discussed and refers to the ideal sampling for soils.

2. Experiment

2.1. Experimental setup

We used an Nd:YAG laser (Diva II, THALES) delivering 10-ns pulses at 1064 nm. The sample received 20 mJ per laser pulse at a repetition rate of 10 Hz. The laser was focused onto the sample with a fused silica lens of 50-mm focal length. The plasma emission was collimated by a parabolic mirror (38.1-mm focal length) and then injected by a 75-mm lens into a 200-μm core optical fiber. This fiber was connected to an Echelle spectrometer (Aryelle, LTB) equipped with a CCD camera (Andor Technology). The spectral range was 282–765 nm with a resolution power better than 10,000. Spectra were accumulated over 50 laser shots on a single position of the sample. The effective time delay between the laser shot and the recording of the spectrum is close to 1 μs in order to optimize the signal/background ratio. In this setup, the spectrometer is the master for triggering control. The CCD camera stays open during 5 s

Table 1
Data set of 220 LIBS measurements. 22 soils samples were measured 10 times each

	Soil name	Abbrev. names	Geological type	Concentration in chromium (ppm)
1	BAglae	BA_1–BA_10	Black clay	2230
2	51	51_1–51_10	Silicate rocks	176
3	52	52_1–52_10	Silicate rocks	168
4	53	53_1–53_10	Silicate rocks	146
5	1900a	1900a_1–1900a_10	Dark calcareous clay	59
6	1901a	1901a_1–1901a_10	Black calcareous clay with sand	27
7	1910b	1910b_1–1910b_10	Brown grey calcareous clay	190
8	2029a	2029a _1–2029a _10	Brown alluvium	22
9	2029c	2029c _1–2029c _10	Sand and clayey gravel	10
10	5270c	5270c _1–5270c _10	Beige sand and big gravel	19
11	5297b	5297b _1–5297b _10	Black sand and gravel	33
12	5744a	5744a _1–5744a _10	Dark clay	38
13	5762d	5762d _1–5762d _10	Beige/grey sand and gravel	5
14	Kaolinite	Kao0_1–kao0_10	White clay	0
15	Kaolinite doped with chromium (50 ppm)	kao50_1–kao50_10	White clay	50
16	Kaolinite doped with chromium (100 ppm)	kao100_1–kao100_10	White clay	100
17	Kaolinite doped with chromium (300 ppm)	kao300_1–kao300_10	White clay	300
18	Kaolinite doped with chromium (500 ppm)	kao500_1–kao500_10	White clay	500
19	Bourran doped with chromium (50 ppm)	Bourran50_1–Bourran50_10	Ochre agricultural soil (28% sand)	116[a]
20	Bourran doped with chromium (100 ppm)	Bourran100_1–Bourran100_10	Ochre agricultural soil (28% sand)	166[a]
21	Bourran doped with chromium (200 ppm)	Bourran200_1–Bourran200_10	Ochre agricultural soil (28% sand)	266[a]
22	Bourran doped with chromium (500 ppm)	Bourran500_1–Bourran500_10	Ochre agricultural soil (28% sand)	566[a]

[a] The soil named Bourran initially contains 66 ppm of chromium. The quantities of 50, 100, 200 and 500 ppm have been added by sorption to this initial value.

and a mechanical chopper provides the optimized temporal window. Thus, each spectrum corresponds to the plasma emission from an adjustable starting time and is integrated over its lifetime. All LIBS spectra are background-corrected via a similar data acquisition with the laser switched off.

2.2. Samples and data sets

The samples were soils prepared as pressed pellets under a pressure of 250 kg/cm^2 during 5 min. Real soils extracted from industrial sites were provided by ANTEA and BRGM and characterized elsewhere by ICP-AES. In addition, laboratory-prepared soils were provided by the IPREM laboratory, doped by sorption with additional amounts of chromium and also characterized by ICP-AES. For this work, 22 different soil samples have been analyzed. Ten LIBS spectra were recorded for each sample, leading to a total number of 220 LIBS spectra to analyze. Details of the samples are given in Table 1.

2.3. Data pretreatment

Regarding blindly at the LIBS spectra related to the data set given in Table 1, it appears that neither a spectral line, nor the full spectrum area can lead to a correct internal normalization, valid for all samples. On the one hand, normalization with respect to a spectral line from a major element for soils such as aluminum or silicon is not convenient because their concentrations vary significantly from one soil to the other. On the other hand, normalization with respect to the full spectrum area is not convenient either. Indeed, this latter option is well suited in the case of on-line control where the matrix of the sample is almost unchanged. Conversely, the matrix is very different from one soil to the other and thus cannot be used to normalize the data.

To normalize the raw LIBS data, a reduced spectral window was chosen regarding the absence of any spectral line in order to have access to the continuum emission. Finally, as a pretreatment, each raw LIBS spectrum was divided by the value of the area calculated from the window 752–755 nm. In this window, the low signal is due to the Bremsstrahlung and is related to experimental parameters, particularly the laser fluence [21].

2.4. Quantitative data analysis

In the framework of environmental analysis, we have especially worked on the detection of chromium in soil samples. Table 1 (right column) gives the actual concentrations of chromium (measured by ICP-AES) for each soil.

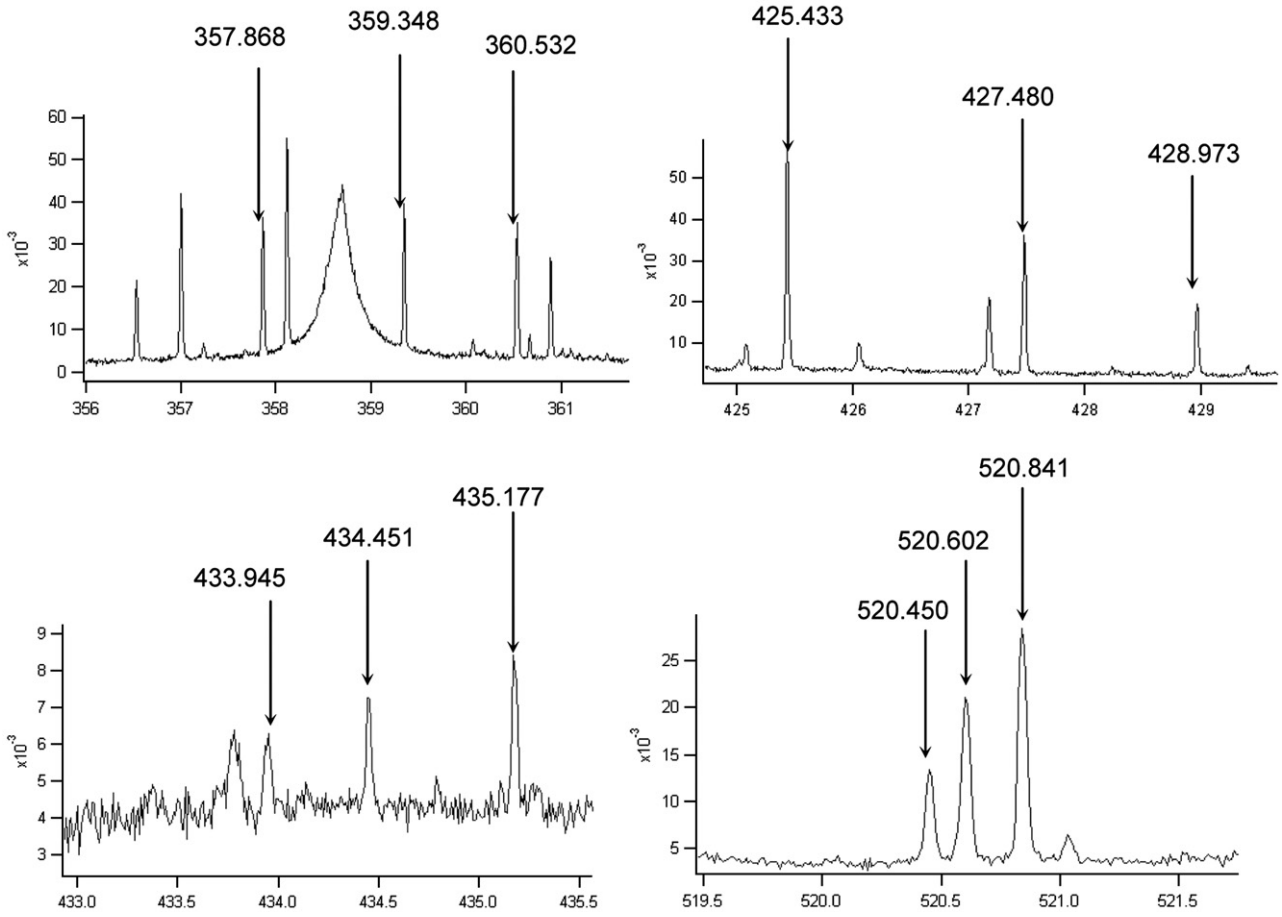

Fig. 1. Extracts of a LIBS spectrum of kaolinite doped with chromium (here kao500). Horizontal axes represent the wavelength in nanometers and vertical axes, the LIBS signal in arbitrary units. Arrows correspond to the 12 selected emission lines of chromium.

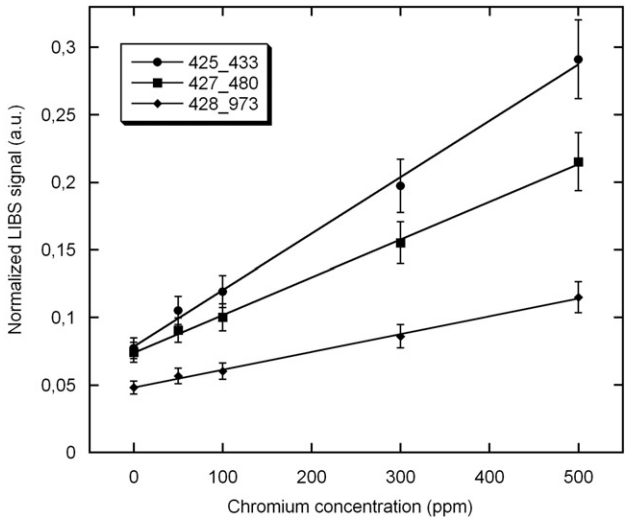

Fig. 2. Calibration curves for chromium inside kaolinite samples. Circles—425.433 nm line, squares—427.480 nm line, diamonds—428.973 nm line. Error bars report relative standard deviations ranging between 3% and 12% (10 measurements per concentration). Lines are linear fits giving regression coefficients greater than 0.996 in the three cases.

The kaolinite samples were doped with chromium up to 500 ppm in order to build a calibration curve and to perform quantitative analysis.

Thanks to the very high resolution of the Aryelle spectrometer (LTB Berlin), it was easy to select 12 spectral lines for chromium (see Fig. 1 for details). It appears that among these 12 lines, the 3 lines at 433.945 nm, 434.451 nm and 435.177 nm are characterized by a S/N ratio much smaller than those of the other ones. As a consequence, they have been rejected and finally only the 9 other lines have been kept for quantitative analysis.

To illustrate the effects of the normalization of raw LIBS data using the spectral window 752–755 nm, let us consider the soil sample named kao500 in Table 1, which is kaolinite doped with chromium at 500 ppm. If one calculates the area under the peak at 520.452 nm – one of the emission lines of chromium – for each of the 10 spectra recorded for this sample, the resulting relative dispersion of these values is around 18% for raw data and it falls to 12% after this normalization. This reduction was observed for all the emission lines and for all the samples reported in Table 1. It is not as efficient as one could wish but, regarding the data set, it provides anyway an enhancement of the treatment by partially compensating the spectral fluctuations.

Let us now consider the set of kaolinite samples (kao0 to kao500). Keeping in mind that 10 LIBS experiments were repeated for each sample, we have calculated 5 new spectra, each being the average over the 10 measurements. Finally, different univariate calibration curves have been plotted in order to test each of the 9 selected lines of chromium. Fig. 2 represents the calibration curves retrieved from 3 of the 9 selected lines of chromium and the corresponding linear fittings.

Fig. 2 displays average values for each spectral line and each concentration. However, it is noted that the relative standard deviation (RSD) of the initial data set is between 3% and 12%, whatever the spectral line and concentration.

Regarding the slopes of these 9 calibration curves, the highest slope is obtained for the line at 425.433 nm (Fig. 2) and the intensity of this line is also the highest. This indicates that this line is the most sensitive and should be preferred in order to obtain a better accuracy in quantitative analysis. However, it must be also verified that there is no overlap between the chromium line at 425.433 nm and other lines related to other chemical elements. This condition has been verified to be correct for all of the soils mentioned in Table 1. Consequently, quantitative analyses of chromium in soil were performed via the calculation of the area of this line.

Now, let us try to use the calibration curve displayed in Fig. 2 (circles), deduced from the chromium line at 425.433 nm. The idea is to demonstrate that a calibration curve obtained for a given matrix of soil cannot be used to get quantitative information for a soil of different matrix. This point has been addressed as described below.

Fig. 3 displays the 425.433 nm line area averaged over the 10 spectra as a function of the concentration in chromium. The calibration curve obtained for kaolinite can be linearly fitted with a regression coefficient better than 0.999. Several soil samples are also represented to demonstrate the matrix effects. Indeed, it is easy to check that the calibration curve of kaolinite cannot be used to predict the concentration in chromium of most of the samples. But, recalling that all the points displayed in Fig. 3 are the result of an average over 10 LIBS measurements, it is necessary to have a look at the relative standard deviation (RSD) of the original data around the mean values. Indeed, except for kaolinite which is related to a small value of RSD (between 3% and 12%), the values of the other soils are widely dispersed (RSD up to 60%). This high dispersion will be discussed in the next section. Consequently, taking into account

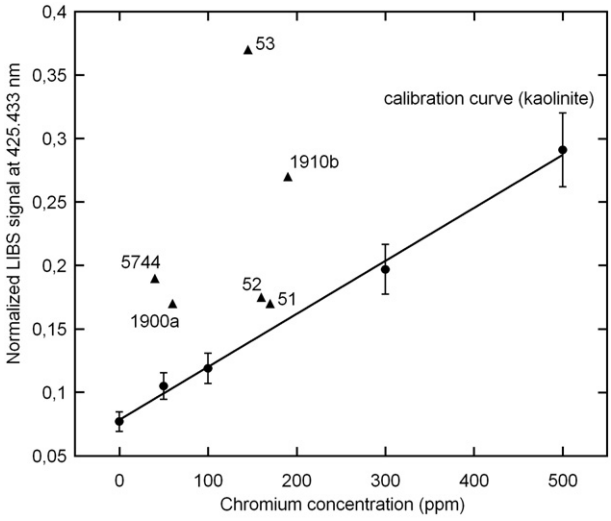

Fig. 3. The LIBS signal at 425.433 nm is plotted as a function of the concentration in chromium for kaolinite samples (circles) and for several other soil samples (triangles) named 51, 52, 53, 1900a, 1910b, and 5744a (cf. Table 1). The line corresponds to a linear fit with a regression coefficient better than 0.999.

the RSD values, one can accept that the samples named 51 and 52 are finally relatively close to the calibration curve. Thus, for these two samples, the calibration curve for kaolinite allows one to predict concentrations of chromium not so far from the actual values. Conversely, if one considers for example the sample named 5744a, averaged over 10 experiments, the predicted concentration, retrieved from the calibration curve of kaolinite, would be very close to 300 ppm while the actual value for this sample is only 38 ppm.

Until now, this work demonstrates that a calibration curve retrieved with a given soil cannot be used to quantitatively analyze another one. Indeed, the physical and chemical properties are very different from one soil to the other; the composition of the major elements varies significantly as well as the size of the grains, the color and many other parameters. This result is very important in the framework of soils analysis by LIBS. As a consequence, it seems to be necessary to build not only one calibration curve but many, one for each soil. Of course, this work is enormous and the only way to go further is to try to sort the different soils into classes, assuming that, for a given class of soils, a specific calibration curve could be used. In the next section, we present results about a method of classification of soils through their LIBS spectra.

2.5. Classification of the samples

As explained in the previous section, a single calibration curve does not allow one to predict the right concentrations in soils by LIBS. So, we present here a method for sorting the LIBS data as a preliminary step to quantitative analysis.

This method is based on Principal Components Analysis (PCA), a multi-linear technique enabling to visualize a series of high-dimensional observations [22].

The experimental data are organized as a matrix where each row corresponds to a new experiment and where the relevant parameters for each experiment – called observations – are displayed in a series of columns. Then, from this original dataset, PCA calculates a linear combination of the observables – commonly the intensities at the different wavelengths – in order to describe the maximum of the covariance, giving the so-called principal components. When the original data are broadband LIBS spectra, it is easy to understand that the contributions of noise and continuous background are widely represented. As a consequence, the first components of PCA calculated from maximum covariance between the data are strongly related to both the noise and the continuum. But, for a good LIBS data processing, exactly the opposite is expected, i.e. the first principal component should be related only to specific relevant emission lines allowing the sorting of the samples. Consequently, we have decided to reduce the data set and to extract only a few data points from our LIBS spectra initially containing more than 50,000 points. For that, one has to decide how to select the few relevant wavelengths.

In the framework of soils analysis, this selection of relevant wavelengths must be connected to the major differences between one soil and another. Of course, the biggest differences between soils come from their composition in major elements, i.e. the chemical elements which compose the matrix. We have then selected in our LIBS spectra 4 lines for aluminum, 3 for silicon, 31 for iron, 10 for calcium, 4 for magnesium, 3 for potassium, 11 for titanium and 2 for manganese. Then each LIBS spectrum is reduced to the areas of these 68 lines (which form the new observations), related to the most relevant chemical elements to separate the different soils into classes.

To calculate the principal components of a series of LIBS data, we have used the commercial software SIMCA-P 11.0 (Umetrics). As detailed above, the number of columns of the input matrix was reduced to 68 – the major chemical elements in soils – and the number of rows was 220, which is exactly the number of LIBS experiments.

Fig. 4 displays the results of PCA over 220 observations and 68 variables. This analysis has been done blindly over the whole data set and the name of each sample has been disclosed only as a post-treatment in order to give physical interpretations to the

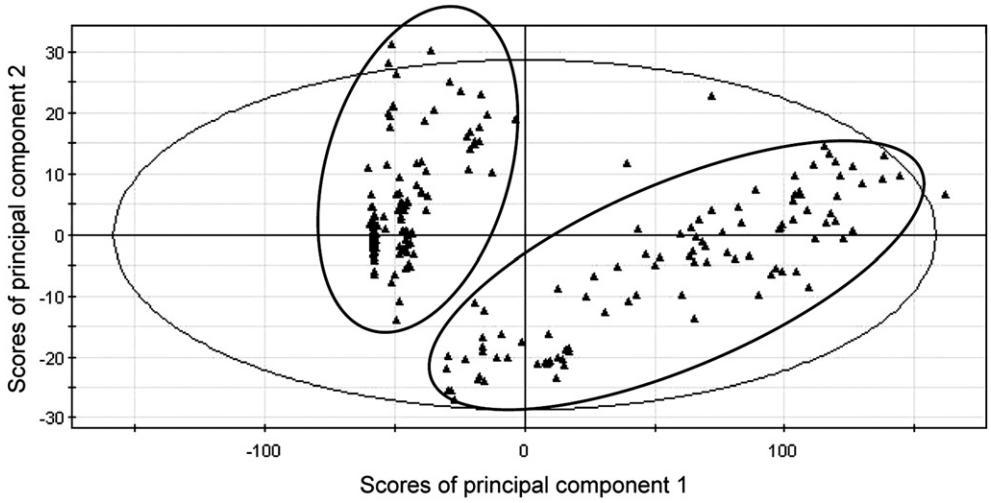

Fig. 4. PC Scores plot, i.e. projection of the experimental LIBS soils data onto the first two principal components. The two scores (t_1/horizontal, t_2/vertical) describe 97% of the variance in the data. The small ellipses demonstrate two different classes.

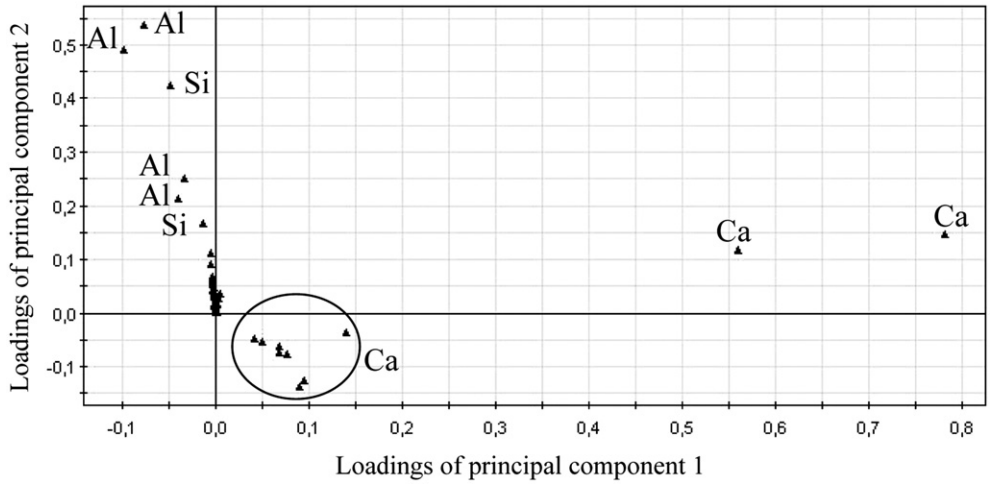

Fig. 5. Loading plot along the first two principal components. This plot shows how the variables are correlated to the principal components. The major contribution to the first component (horizontal axis) comes from calcium while the second component (vertical axis) is essentially related to aluminum and silicon.

results. Two groups of points are easily separated. Ellipses have been plotted for better clarity; the left one is composed of LIBS data retrieved from the samples kaolinite, 51, 52, 53 and Bourran and the right one contains the samples 1900a, 1901a, 5744a, 5270c, 5762a, 2029a, BAglae, 5297b, 2029a, 2029c. When looking simultaneously at the scores (Fig. 4) and at the corresponding so-called loadings (Fig. 5) for this PCA, one can understand that the first (horizontal) scores direction is sensitive to the concentration in calcium while the second (vertical) one is sensitive to the concentrations in aluminum and silicon. Indeed, the loadings of the first principal component are mainly the result of the selected emission lines of calcium. Consequently, a sample having a large concentration in calcium corresponds to a point located on the right side of the scores plot (Fig. 4). Conversely, it is easy to understand that the samples depicted on the left side of Fig. 4 have the lowest concentration in calcium.

The next step consists in new PCAs applied to each of the identified classes. Fig. 6 displays the first two components of a PCA applied to the class containing kaolinite, 51, 52, 53 and Bourran (the left ellipse in Fig. 4). A sub-class is clearly identified, containing only kaolinite samples. This result is particularly interesting since we can now define a criterion of spectral similarity, allowing us to use a given calibration line for quantitative analysis. In our case, if an unknown spectrum being successively analyzed by the two PCAs (Fig. 4 and 6) was close to the kaolinite spectra, we could reasonably measure its chromium concentration from the calibration curve of kaolinite (Fig. 3) without making a big error. This methodology opens the way to quantitative analysis by LIBS, even when the dataset is composed of samples related to different matrices.

On Fig. 6 again, the first component is related to calcium and the second one to aluminum. Thus, the kaolinite samples which do not contain calcium are located at the left end of the distribution and well separated from the other samples. In addition, it appears that the points corresponding to the kaolinite samples are much less dispersed than the other ones. This is due to the nature of the soil samples. Kaolinite is a very homogeneous white clay used as a reference soil. It is not

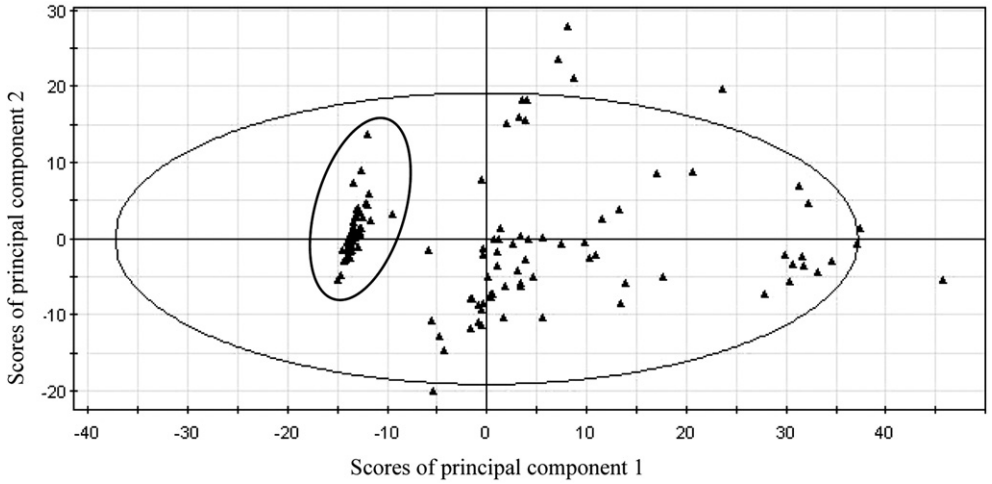

Fig. 6. PC scores, i.e. projection of the experimental LIBS soils data extracted from the class containing kaolinite, 51, 52, 53 and Bourran. The two scores (t_1/horizontal, t_2/vertical) describe 89% of the variance in the data. The small ellipse indicates the sub-class of kaolinite samples.

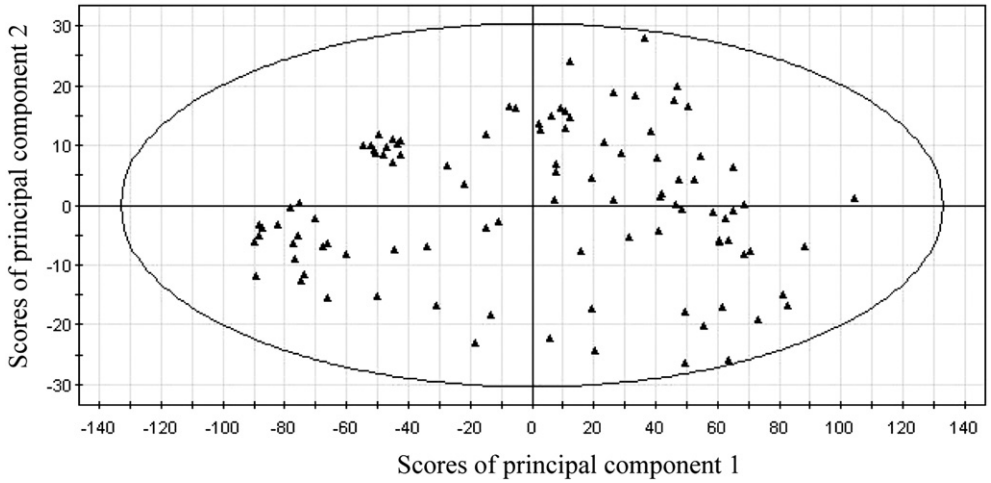

Fig. 7. PC scores plot, i.e. projection of the LIBS spectra of a part of the soils (see the text) onto the first two principal components. The two scores (t_1/horizontal, t_2/vertical) describe 98% of the variance in the data.

surprising to observe a small dispersion of the related points in Fig. 6. Even more, one would expect a smaller dispersion, as small on the vertical direction (mainly influenced by aluminum) as on the horizontal one (mainly influenced by calcium). But in fact, there is no calcium in kaolinite while aluminum is a major element. The remaining dispersion on the vertical axis reveals that the normalization chosen here, i.e. a normalization using the spectral window 752–755 nm as explained before, is not perfectly suited for the aluminum lines. Indeed, the four lines selected for aluminum (308.215, 309.283, 394.400 and 396.152 nm), not displayed here, are enlarged, as one can observe in the case of self-absorption into optically thick plasma and they are very sensitive to the experimental conditions. At the opposite, the lines of chromium depicted in Fig. 2 are narrow and exhibit a very small dispersion regarding the area under the peak, used for quantification; this is why the linear fitting of the kaolinite data is excellent (Fig. 3).

One can observe a very large dispersion of the remaining points in Fig. 6. This dispersion is much higher in the case of real heterogeneous soils than in the case of kaolinite, which is a very homogeneous soil used as a reference. Heterogeneity of soils can even be seen with the naked eye; real soils exhibits grains of different colors and different sizes with also the presence of clusters. Consequently, even if each LIBS spectrum is the result of an average over 50 laser shots, it is not surprising that the heterogeneities of the samples lead to a large dispersion of the data. This high dispersion of data is clearly a limit for PCA and thus for classification.

To finish, let us consider now the class containing the series of remaining soils: BAglae, 1900a, 1901a, 1910b, 2029a, 2029c, 5270c, 5297b, 5744a, 5762a (right ellipse in Fig. 4). The result of PCA is depicted on Fig. 7.

In this case, no class can be distinguished probably because of the high dispersion of the data due to heterogeneities of these soil samples. The first two principal components are mainly related to calcium as one can verify by looking at the loadings in the same way as in Fig. 6. The small dense cloud of points visible in the left up sector of Fig. 7 is mainly composed of data related to the sample named BAglae. However, there are also included in this group of points the samples 5744a_10 and 1900a_7. So this group of points does not correspond to a pure class of samples.

In conclusion, the poor ability of classifying soil samples by PCA regarding their LIBS spectra is disappointing. Indeed, when one knows that a direct quantitative analysis is not possible because of important matrix effects, a preliminary classification was announced to be a necessary step before quantitative analysis. We still believe that this is the right way of working with soil samples but the large dispersion of data that has been observed makes us think that a specific work has to be done concerning the sampling of soils. Indeed, because of important heterogeneities, the spectral data collected for a given soil exhibit a large dispersion. These heterogeneities are real and would have lead to the same kind of dispersion even with other space-resolved analytical techniques, such as LA-ICP for example. So, it does not mean that LIBS is not a suitable analytical method to deal with soil samples but that, whatever the analytical technique (LIBS, ICP,...), the step of sampling still remains essential to reach quantitative information on soil samples.

3. Conclusion

We demonstrated that LIBS signals for soil samples are strongly affected by the matrix effects and that a classification of data is necessary as a preliminary step of a quantitative analysis. A data set containing 220 LIBS spectra was blindly analyzed by a series of Principal Components Analyzes (PCA). As a pre-processing, a reduction of the dimensionality of the original dataset was achieved by selecting a reduced number (68) of emission lines corresponding to the major chemical elements in the soils. Even if PCA is known to be a very efficient method for sorting and classifying the data, we demonstrated its limits due to the nature of the soil samples, i.e. the very high variation of the physical and chemical parameters. Finally, besides the analysis of the LIBS data, the sampling

appeared as a key point for future work on soils analysis. This very important feature will be addressed in future work in collaboration with BRGM (Bureau de Recherche Géologique et Minière). In addition, further studies on the basis of experimental design will be carried out in collaboration with IPREM (Institut Pluridisciplinaire de Recherche sur l'Environnement et les Matériaux) with the objective of going towards a LIBS database for soils.

These future prospects on LIBS applied to soil analysis are part of a collaborative program called SOLSTICE which has received the financial support of ANR (Agence Nationale de la Recherche), the French Agency for Research.

Acknowledgements

The authors gratefully acknowledge Isabelle Le Hecho, Sylvaine Tellier and Martine Potin-Gautier from IPREM (Institut Pluridisciplinaire de Recherche sur l'Environnement et les Matériaux) for the laboratory-prepared soils samples with specific concentration of chromium, Stéphane Roy and Karine Le Pierrès from BRGM (Bureau de Recherche Géologique et Minière) for providing real soil samples and ANTEA company for providing also real soil samples. They also acknowledge the CNRS (Centre National de la Recherche Scientifique), the ADEME (Agence de l'Environnement et de la Maîtrise de l'Energie), the Conseil Régional d'Aquitaine and the ANR (Agence National de la Recherche) for their financial support.

References

[1] A.W. Miziolek, V. Palleschi, I. Schechter, Laser-Induced Breakdown Spectroscopy (LIBS) Fundamentals and Applications, Cambridge University Press, New York, 2006.
[2] D.A. Cremers, L.J. Radziemski, Handbook of Laser-Induced Breakdown Spectroscopy, John Wiley & Sons, Ltd, England, 2006.
[3] M.Z. Martin, N. Labbé, T.G. Rials, S.D. Wullschleger, Analysis of preservative-treated wood by multivariate analysis of laser-induced breakdown spectroscopy spectra, Spectrochim. Acta Part B 60 (2005) 1179–1185.
[4] J. Amador-Hernández, L.E. García-Ayuso, J.M. Fernández-Romero, M.D. Luque de Castro, Partial least squares regression for problem solving in precious metal analysis by laser induced breakdown spectrometry, J. Anal. At. Spectrom. 6 (2000) 587–593.
[5] M. Kraushaar, R. Noll, H.-U. Schmitz, Slag analysis with laser-induced breakdown spectrometry, Appl. Spectrosc. 57 (2003) 1282–1287.
[6] J.-B. Sirven, B. Bousquet, L. Canioni, L. Sarger, Laser-induced breakdown spectroscopy of composite samples: comparison of advanced chemometrics methods, Anal. Chem. 78 (2006) 1462–1469.
[7] J.-B. Sirven, B. Bousquet, L. Canioni, L. Sarger, S. Tellier, M. Potin-Gautier, I. Le Hecho, Qualitative and quantitative investigation of chromium-polluted soils by laser-induced breakdown spectroscopy combined with neural networks analysis, Anal. Bioanal. Chem. 385 (2006) 256–262.
[8] T.M. Moskal, D.W. Hahn, On-line sorting of wood treated with chromated copper arsenate using laser-induced breakdown spectroscopy, Appl. Spectrosc. 56 (2002) 1337–1344.
[9] J.M. Anzano, I.B. Gornushkin, B.W. Smith, J.D. Winefordner, Laser-induced plasma spectroscopy for plastic identification, Polym. Eng. Sci. 40 (2000) 2423–2429.
[10] A. Kumar, F.-Y. Yueh, J.P. Singh, S. Burgess, Characterization of malignant tissue cells by laser-induced breakdown spectroscopy, Appl. Opt. 43 (2004) 5399–5403.
[11] T. Kim, Z.G. Specht, P.S. Vary, C.T. Lin, Spectral fingerprints of bacterial strains by laser-induced breakdown spectroscopy, J. Phys. Chem., B 108 (2004) 5477–5482.
[12] S. Morel, N. Leone, P. Adam, J. Amouroux, Detection of bacteria by time-resolved laser-induced breakdown spectroscopy, Appl. Opt. 42 (2003) 6184–6191.
[13] R. Sattmann, I. Mönch, H. Krause, R. Noll, S. Couris, A. Hatziapostolou, A. Mavromanolakis, C. Fotakis, E. Larrauri, R. Miguel, Laser-induced breakdown spectroscopy for polymer identification, Appl. Spectrosc. 52 (1998) 456–461.
[14] M.J. Adams, Chemometrics in analytical spectroscopy. RSC Analytical Spectroscopy Monographs, 2nd editionRoyal Society of Chemistry, Cambridge, 2004.
[15] H. Fink, U. Panne, R. Niessner, Process analysis of recycled thermoplasts from consumer electronics by laser-induced plasma spectroscopy, Anal. Chem. 74 (2002) 4334–4342.
[16] S.R. Goode, S.L. Morgan, R. Hoskins, A. Oxsher, Identifying alloys by laser-induced breakdown spectroscopy with a time resolved high resolution echelle spectrometer, J. Anal. At. Spectrom. 9 (2000) 1133–1138.
[17] Ota Samek, Helmut H. Telle, David C.S. Beddows, Laser-induced breakdown spectroscopy: a tool for real-time, in vitro and in vivo identification of carious teeth, BMC Oral Health 1 (2001).
[18] A.C. Samuels, F.C. De Lucia Jr., K.L. Mc Nesby, A.W. Miziolek, Laser-induced breakdown spectroscopy of bacterial spores, molds, pollens, and protein: initial studies of discrimination potential, Appl. Opt. 42 (2003) 6205–6209.
[19] C.A. Munson, F.C. De Lucia Jr., T. Piehler, K.L. Mc Nesby, A.W. Miziolek, Investigation of statistics strategies for improving the discriminating power of laser-induced breakdown spectroscopy for chemical and biological warfare agent simulants, Spectrochim. Acta Part B 60 (2005) 1217–1224.
[20] J.D. Hybl, G.A. Lithgow, S.G. Buckley, Laser-induced breakdown spectroscopy detection and classification of biological aerosols, Appl. Spectrosc. 57 (2003) 1207–1215.
[21] J.-B. Sirven, B. Bousquet, L. Canioni, L. Sarger, Time-resolved and time-integrated single-shot laser-induced plasma experiments using nanosecond and femtosecond laser pulses, Spectrochim. Acta Part B 59 (2004) 1033–1039.
[22] H. Martens, T. Næs, Multivariate calibration, John Wiley & Sons, Chichester, New-York, 1989.